

Shape Adaptation for 3D Hairstyle Retargeting

SUPPLEMENTAL MATERIAL

Lu Yu Zhong Ren Youyi Zheng Xiang Chen Kun Zhou

State Key Lab of CAD&CG, Zhejiang University

1 Formula Derivation for Embedded Membrane Deformation

We need the Jacobian and Hessian of the energy to employ Projected Newton for minimizing Equation 15 in the main text. In the following sections, we introduce how to compute these two quantities. To simplify the discussion, we will only consider a single triangle.

Suppose the intrinsic parameters and 3D coordinates of the three triangle vertices are $\mathbf{u}_0, \mathbf{u}_1, \mathbf{u}_2$ and $\mathbf{x}_0, \mathbf{x}_1, \mathbf{x}_2$. Now, we stack them to obtain

$$\mathbf{u} = \begin{bmatrix} \mathbf{u}_0 \\ \mathbf{u}_1 \\ \mathbf{u}_2 \end{bmatrix}, \quad \mathbf{x} = \begin{bmatrix} \mathbf{x}_0 \\ \mathbf{x}_1 \\ \mathbf{x}_2 \end{bmatrix}, \quad (1)$$

and we should compute $\frac{\partial \psi}{\partial \mathbf{u}}$ and $\frac{\partial^2 \psi}{\partial \mathbf{u}^2}$. Here, we choose the neo-Hookean membrane model as the strain energy density function ψ :

$$\psi(\mathbf{F}) = \frac{\mu}{2}(\text{tr}(\mathbf{F}^T \mathbf{F}) - 2) - \mu \log(J) + \frac{\lambda}{2} \log^2(J), \quad (2)$$

where \mathbf{F} is deformation gradient and $J = \det(\mathbf{F})$. The parameters μ and λ are related to Young's modulus E and Poisson's ratio ν via

$$\mu = \frac{E}{2(1 + \nu)}, \quad \lambda = \frac{E\nu}{(1 + \nu)(1 - 2\nu)}. \quad (3)$$

1.1 Computation of the Jacobian $\frac{\partial \psi}{\partial \mathbf{u}}$

By the chain rule, we have

$$\frac{\partial \psi}{\partial \mathbf{u}} = \frac{\partial \psi}{\partial \mathbf{F}} \frac{\partial \mathbf{F}}{\partial \mathbf{x}} \frac{\partial \mathbf{x}}{\partial \mathbf{u}}. \quad (4)$$

1.1.1 Computation of $\frac{\partial \mathbf{x}}{\partial \mathbf{u}}$

With Equation 18 and Equation 19 in the main text, we have

$$\frac{\partial \mathbf{x}_i}{\partial \mathbf{u}_i} = [\mathbf{X}_1^{\tau_i} - \mathbf{X}_0^{\tau_i} \mid \mathbf{X}_2^{\tau_i} - \mathbf{X}_0^{\tau_i}] [\mathbf{u}_1^{\tau_i} - \mathbf{u}_0^{\tau_i} \mid \mathbf{u}_2^{\tau_i} - \mathbf{u}_0^{\tau_i}]^{-1}, \quad \forall i \in \{0, 1, 2\}, \quad (5)$$

where τ_i is the triangle (of the head mesh \mathcal{H}) inside which the vertex i locates. Then, we can obtain

$$\frac{\partial \mathbf{x}}{\partial \mathbf{u}} = \begin{bmatrix} \frac{\partial \mathbf{x}_0}{\partial \mathbf{u}_0} & & \\ & \frac{\partial \mathbf{x}_1}{\partial \mathbf{u}_1} & \\ & & \frac{\partial \mathbf{x}_2}{\partial \mathbf{u}_2} \end{bmatrix}. \quad (6)$$

1.1.2 Computation of $\frac{\partial \mathbf{F}}{\partial \mathbf{x}}$

As shown in Section 6.1 of the main text, $\mathbf{F} = [\mathbf{x}_1 - \mathbf{x}_0 \mid \mathbf{x}_2 - \mathbf{x}_0] \mathbf{D}^{-1}$, where \mathbf{D}^{-1} is a constant 2×2 matrix computed with the undeformed triangle. For convenience, we denote $\mathbf{D}^{-1} = \begin{bmatrix} d_{00} & d_{01} \\ d_{10} & d_{11} \end{bmatrix}$ and express \mathbf{F} as a vector $\in \mathbb{R}^6$ by stacking its three rows. Then $\frac{\partial \mathbf{F}}{\partial \mathbf{x}}$ can be computed as:

$$\frac{\partial \mathbf{F}}{\partial \mathbf{x}} = \begin{bmatrix} -(d_{00} + d_{10}) & 0 & 0 & d_{00} & 0 & 0 & d_{10} & 0 & 0 \\ -(d_{01} + d_{11}) & 0 & 0 & d_{01} & 0 & 0 & d_{11} & 0 & 0 \\ 0 & -(d_{00} + d_{10}) & 0 & 0 & d_{00} & 0 & 0 & d_{10} & 0 \\ 0 & -(d_{01} + d_{11}) & 0 & 0 & d_{01} & 0 & 0 & d_{11} & 0 \\ 0 & 0 & -(d_{00} + d_{10}) & 0 & 0 & d_{00} & 0 & 0 & d_{10} \\ 0 & 0 & -(d_{01} + d_{11}) & 0 & 0 & d_{01} & 0 & 0 & d_{11} \end{bmatrix}. \quad (7)$$

1.1.3 Computation of $\frac{d\psi}{d\mathbf{F}}$

As shown in [1], for a deformation gradient $\mathbf{F} \in \mathbb{R}^{3 \times 2}$, its Polar SVD is $\mathbf{F} = \mathbf{U}\Sigma\mathbf{V}^T$, where

$$\mathbf{U} = [\mathbf{U}_0 \mid \mathbf{U}_1 \mid \mathbf{U}_2] \in \mathbb{R}^{3 \times 3}, \quad \Sigma = \begin{bmatrix} \sigma_0 & 0 \\ 0 & \sigma_1 \\ 0 & 0 \end{bmatrix} \in \mathbb{R}^{3 \times 2}, \quad \mathbf{V} = [\mathbf{V}_0 \mid \mathbf{V}_1] \in \mathbb{R}^{2 \times 2}. \quad (8)$$

Then $\frac{\partial \psi}{\partial \mathbf{F}}$ can be computed as

$$\frac{\partial \psi}{\partial \mathbf{F}} = \mathbf{U} \begin{bmatrix} \frac{\partial \hat{\psi}}{\partial \sigma_0} & 0 \\ 0 & \frac{\partial \hat{\psi}}{\partial \sigma_1} \\ 0 & 0 \end{bmatrix} \mathbf{V}^T, \quad (9)$$

where $\hat{\psi}$ is expressed as

$$\hat{\psi}(\sigma_0, \sigma_1) = \psi(\mathbf{F}) = \frac{\mu}{2}((\sigma_0 + \sigma_1) - 2) - \mu \log(\sigma_0 \sigma_1) + \frac{\lambda}{2} \log^2(\sigma_0 \sigma_1). \quad (10)$$

Note that $\frac{\partial \hat{\psi}}{\partial \sigma_0}$ and $\frac{\partial \hat{\psi}}{\partial \sigma_1}$ can be readily computed via Equation (10).

1.2 Computation of the Hessian $\frac{\partial^2 \psi}{\partial \mathbf{u}^2}$

As shown in Section 1.1.1 and 1.1.2, both $\frac{\partial \mathbf{x}}{\partial \mathbf{u}}$ and $\frac{\partial \mathbf{F}}{\partial \mathbf{x}}$ are constant matrices (independent of \mathbf{u}), so we set a constant matrix $\mathbf{M} = \frac{\partial \mathbf{F}}{\partial \mathbf{x}} \frac{\partial \mathbf{x}}{\partial \mathbf{u}}$. Then we have $\frac{\partial \psi}{\partial \mathbf{u}} = \frac{\partial \psi}{\partial \mathbf{F}} \mathbf{M}$, and by the chain rule:

$$\begin{aligned} \frac{\partial^2 \psi}{\partial \mathbf{u}^2} &= \frac{\partial \left(\mathbf{M}^T \left(\frac{\partial \psi}{\partial \mathbf{F}} \right)^T \right)}{\partial \mathbf{F}} \frac{\partial \mathbf{F}}{\partial \mathbf{x}} \frac{\partial \mathbf{F}}{\partial \mathbf{u}} \\ &= \mathbf{M}^T \frac{\partial^2 \psi}{\partial \mathbf{F}^2} \mathbf{M}. \end{aligned} \quad (11)$$

1.2.1 Computation of $\frac{\partial^2 \psi}{\partial \mathbf{F}^2}$

Following [1], we derive the formula for computing $\frac{\partial^2 \psi}{\partial \mathbf{F}^2}$ by using symbolic computation in MATLAB:

$$\frac{\partial^2 \psi}{\partial \mathbf{F}^2} = \begin{bmatrix} \hat{\psi}_{,\sigma_0\sigma_0} & \hat{\psi}_{,\sigma_0\sigma_1} & 0 & 0 & 0 & 0 \\ \hat{\psi}_{,\sigma_1\sigma_0} & \hat{\psi}_{,\sigma_1\sigma_1} & 0 & 0 & 0 & 0 \\ 0 & 0 & \frac{\lambda \log(\sigma_0\sigma_1) - \mu + \mu\sigma_1^2}{\sigma_1^2} & 0 & 0 & 0 \\ 0 & 0 & 0 & \frac{\lambda \log(\sigma_0\sigma_1) - \mu + \mu\sigma_0^2}{\sigma_0^2} & 0 & 0 \\ 0 & 0 & 0 & 0 & 0 & \mathbf{B} \\ 0 & 0 & 0 & 0 & 0 & 0 \end{bmatrix}, \quad (12)$$

$$\mathbf{B} = \frac{1}{\sigma_0^2 - \sigma_1^2} \begin{bmatrix} \sigma_0 \hat{\psi}_{,\sigma_0} - \sigma_1 \hat{\psi}_{,\sigma_1} & \sigma_1 \hat{\psi}_{,\sigma_0} - \sigma_0 \hat{\psi}_{,\sigma_1} \\ \sigma_1 \hat{\psi}_{,\sigma_0} - \sigma_0 \hat{\psi}_{,\sigma_1} & \sigma_0 \hat{\psi}_{,\sigma_0} - \sigma_1 \hat{\psi}_{,\sigma_1} \end{bmatrix}, \quad (13)$$

where $\hat{\psi}_{,\sigma_i} = \frac{\partial \hat{\psi}}{\partial \sigma_i}$ and $\hat{\psi}_{,\sigma_i\sigma_j} = \frac{\partial^2 \hat{\psi}}{\partial \sigma_i \partial \sigma_j}$, which can be computed via Equation (10).

2 More Retargeting Results

Figure 1 shows the 11 hairstyles mentioned in the main text, all retargeted to the same character. Figure 2 shows more retargeting results with hairline edits.



Figure 1: Retargeting 11 different hairstyles to the same character.

To further justify the efficacy of our embedded membrane formulation, we test two additional parameterization methods, i.e., Harmonic map [2], and the one in [3], for hairline edit. Figure 3 demonstrates that our method outperforms all the alternatives regarding visual fidelities, scalp mesh distortions, and density change errors. Figure 4 compares more scalp mesh distortions under hairline edits.

Table 1 lists the per-task density change error of the hair-root relocation methods. There are a total of 10 hairstyles with 6 hairline edits. The numerical data indicate that our embedded membrane deformation method (under LSCM [4] parameterization) outperforms the other two alternatives (with four different parameterizations) in almost all retargeting tasks.

Our hair-root relocation method is independent of the choice of parameterization. Table 2 lists the L_1 and L_∞ norms of the density change vectors for our method with four different parameterization algorithms. The numerical results remain consistent.

Figure 5 and Table 3 show more qualitative/quantitative comparisons of the multi-scale and global solving strategies. Figure 6 and Figure 7 show more qualitative comparisons to the transfer methods based on 3D RBF and rigid transformation. Table 4 shows the quantitative energy values for the ablation study.

3 Auxiliary Bones for Ears

The narrow space between the ears and the scalp is challenging for some hairstyles and could lead to unnatural results or even artifacts (see Figure 8b). To tackle this problem, we set up several auxiliary bones at the ears (see Figure 8a). These additional reference bones can effectively constrain the hair particles behind the ears to stay at their correct positions (see Figure 8c).

4 Comparison with Industrial Software

Figure 9 shows a comparison of our method with the *Transfer* command of Autodesk Maya [5], which fails to produce a reasonable hairstyle transfer for the target character.

References

- [1] C. Jiang, C. Schroeder, J. Teran, A. Stomakhin, and A. Selle, “The material point method for simulating continuum materials,” in *Acm siggraph 2016 courses*, 2016, pp. 1–52.
- [2] M. Eck, T. DeRose, T. Duchamp, H. Hoppe, M. Lounsbery, and W. Stuetzle, “Multiresolution analysis of arbitrary meshes,” in *Proceedings of the 22nd annual conference on Computer graphics and interactive techniques*, 1995, pp. 173–182.
- [3] L. Wang, Y. Yu, K. Zhou, and B. Guo, “Example-based hair geometry synthesis,” in *ACM SIGGRAPH 2009 papers*, 2009, pp. 1–9.
- [4] B. Lévy, S. Petitjean, N. Ray, and J. Maillot, “Least squares conformal maps for automatic texture atlas generation,” in *Seminal Graphics Papers: Pushing the Boundaries, Volume 2*, 2023, pp. 193–202.
- [5] Autodesk, INC., “Maya.” [Online]. Available: <https://www.autodesk.com/products/maya/overview>
- [6] L. Liu, L. Zhang, Y. Xu, C. Gotsman, and S. J. Gortler, “A local/global approach to mesh parameterization,” in *Computer graphics forum*, vol. 27, no. 5. Wiley Online Library, 2008, pp. 1495–1504.



Figure 2: Retargeting 7 hairstyles to the same character under 6 different hairline edits.

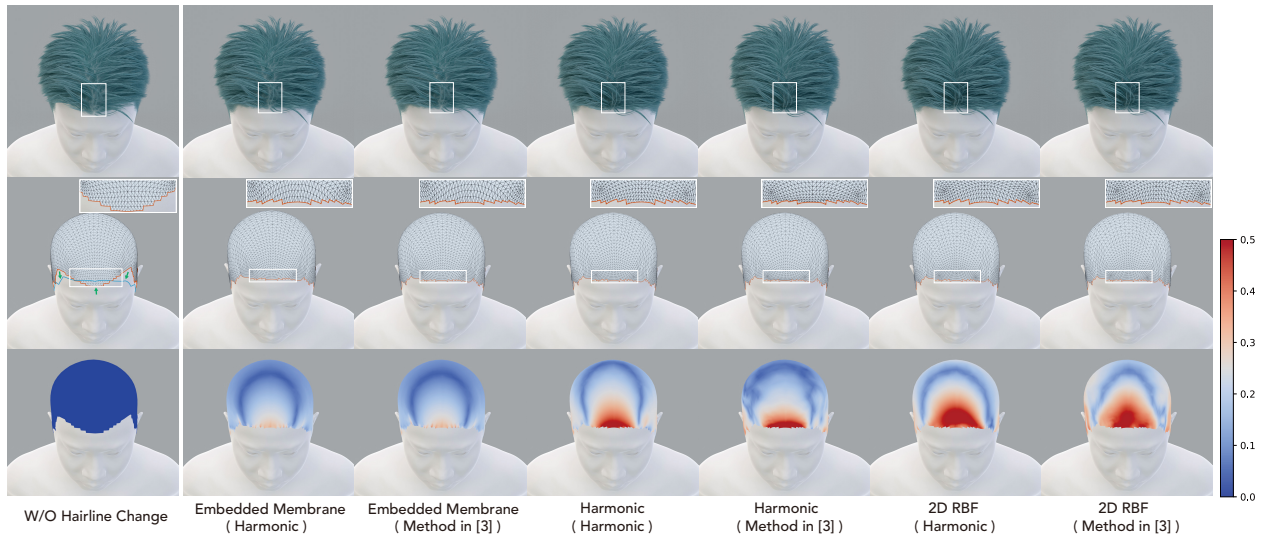


Figure 3: More comparisons of hair-root relocation methods. From up to bottom: the produced 3D hairstyles, the deformed scalp mesh, and the hair-root density changes.

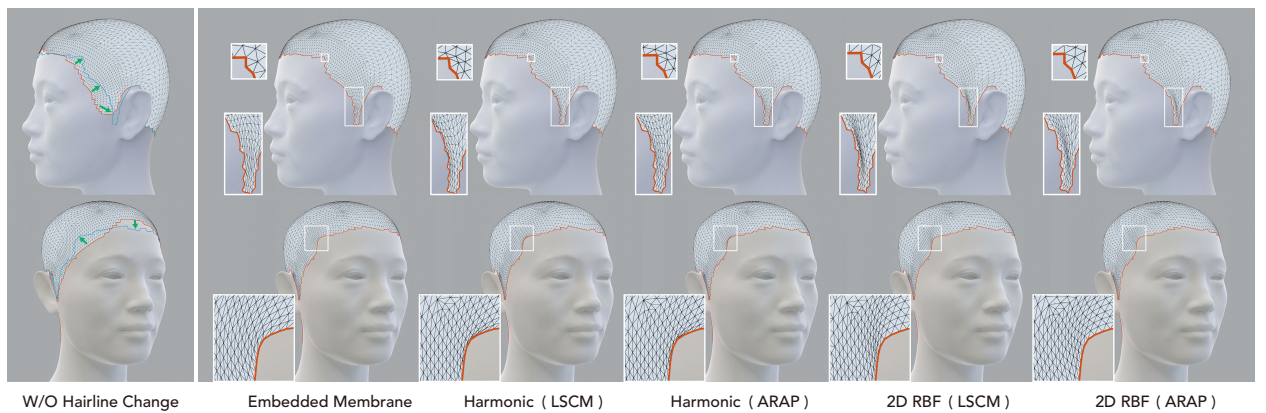


Figure 4: More comparisons of hair-root relocation methods regarding scalp mesh. Note the over-compressions and distortions in columns 2-5.



Figure 5: More comparisons of the global and multi-scale solving strategies. A high-fidelity transfer necessitates the preservation of the inter-strand relationship (ISR). Our multi-scale solving approximates the global solving while providing significant runtime acceleration. See Table 3 for quantitative results.

Table 1: Density changes of the hair roots. For 10 hairstyles under 6 hairline edits, we compare our method and two alternatives, i.e., the 2D harmonic displacements and the 2D RBF-based interpolation, using four different parameterizations, i.e., LSCM [4], Harmonic map [2], ARAP [6] and the one introduced in [3]. We report the L_1 -norm of the density change vectors. Our method produces much smaller distortions in all cases.

Hairline	Hairstyle	Membrane	Harmonic				RBF (2D)			
		LSCM	LSCM	Harmonic	ARAP	Scalp	LSCM	Harmonic	ARAP	Scalp
Straight	Short	0.041	0.087	0.087	0.090	0.088	0.099	0.101	0.111	0.120
Straight	Dreadlocks	0.024	0.047	0.047	0.047	0.046	0.046	0.047	0.044	0.051
Straight	Spiky	0.040	0.120	0.119	0.135	0.168	0.152	0.156	0.150	0.161
Straight	Side fringe	0.046	0.122	0.121	0.142	0.165	0.114	0.114	0.133	0.137
Straight	Long 1	0.040	0.070	0.071	0.079	0.107	0.092	0.092	0.103	0.123
Straight	Long 2	0.015	0.034	0.034	0.033	0.035	0.041	0.041	0.045	0.053
Straight	Ponytail	0.033	0.073	0.073	0.075	0.084	0.076	0.076	0.076	0.098
Straight	Updo 1	0.036	0.058	0.058	0.061	0.086	0.060	0.059	0.066	0.093
Straight	Updo 2	0.048	0.068	0.068	0.076	0.163	0.069	0.070	0.073	0.116
Straight	Med-Len	0.028	0.055	0.055	0.056	0.056	0.061	0.061	0.067	0.069
Bell-shaped	Short	0.034	0.045	0.045	0.050	0.061	0.060	0.058	0.054	0.065
Bell-shaped	Dreadlocks	0.038	0.057	0.057	0.058	0.060	0.051	0.052	0.053	0.056
Bell-shaped	Spiky	0.046	0.066	0.066	0.079	0.108	0.078	0.077	0.080	0.100
Bell-shaped	Side fringe	0.058	0.095	0.095	0.118	0.158	0.089	0.087	0.093	0.103
Bell-shaped	Long 1	0.078	0.122	0.122	0.139	0.220	0.096	0.098	0.096	0.132
Bell-shaped	Long 2	0.045	0.066	0.066	0.070	0.082	0.058	0.058	0.058	0.073
Bell-shaped	Ponytail	0.062	0.097	0.097	0.104	0.133	0.090	0.089	0.091	0.117
Bell-shaped	Updo 1	0.075	0.121	0.121	0.140	0.240	0.113	0.122	0.118	0.157
Bell-shaped	Updo 2	0.091	0.130	0.131	0.147	0.235	0.118	0.124	0.117	0.145
Bell-shaped	Med-Len	0.049	0.069	0.069	0.073	0.078	0.065	0.065	0.073	0.084
Uneven	Short	0.050	0.081	0.081	0.077	0.066	0.127	0.128	0.117	0.087
Uneven	Dreadlocks	0.041	0.061	0.061	0.061	0.059	0.079	0.080	0.066	0.050
Uneven	Spiky	0.045	0.110	0.110	0.110	0.091	0.171	0.177	0.146	0.105
Uneven	Side fringe	0.043	0.104	0.104	0.110	0.097	0.104	0.104	0.112	0.092
Uneven	Long 1	0.021	0.051	0.051	0.054	0.048	0.067	0.071	0.082	0.074
Uneven	Long 2	0.034	0.056	0.056	0.057	0.060	0.062	0.062	0.061	0.055
Uneven	Ponytail	0.040	0.064	0.064	0.061	0.059	0.073	0.075	0.069	0.087
Uneven	Updo 1	0.017	0.036	0.036	0.037	0.038	0.051	0.052	0.055	0.062
Uneven	Updo 2	0.029	0.060	0.061	0.065	0.072	0.072	0.076	0.067	0.068
Uneven	Med-Len	0.050	0.076	0.076	0.079	0.078	0.093	0.093	0.091	0.078
M-shape	Short	0.046	0.064	0.064	0.063	0.059	0.081	0.079	0.082	0.080
M-shape	Dreadlocks	0.032	0.042	0.042	0.042	0.046	0.051	0.050	0.045	0.048
M-shape	Spiky	0.037	0.075	0.075	0.079	0.069	0.102	0.100	0.098	0.090
M-shape	Side fringe	0.048	0.098	0.097	0.109	0.097	0.099	0.096	0.109	0.096
M-shape	Long 1	0.025	0.064	0.064	0.071	0.072	0.078	0.079	0.089	0.086
M-shape	Long 2	0.027	0.041	0.041	0.041	0.042	0.046	0.046	0.044	0.043
M-shape	Ponytail	0.037	0.059	0.059	0.060	0.057	0.078	0.079	0.071	0.089
M-shape	Updo 1	0.026	0.075	0.075	0.081	0.089	0.078	0.079	0.075	0.082
M-shape	Updo 2	0.032	0.056	0.056	0.060	0.071	0.052	0.054	0.053	0.060
M-shape	Med-Len	0.041	0.054	0.054	0.056	0.061	0.059	0.059	0.062	0.063
Triangular	Short	0.053	0.080	0.079	0.078	0.085	0.103	0.102	0.088	0.107
Triangular	Dreadlocks	0.051	0.095	0.095	0.100	0.102	0.098	0.097	0.098	0.114
Triangular	Spiky	0.046	0.117	0.117	0.105	0.099	0.165	0.166	0.121	0.145
Triangular	Side fringe	0.034	0.068	0.068	0.066	0.061	0.063	0.064	0.060	0.086
Triangular	Long 1	0.024	0.058	0.058	0.061	0.063	0.073	0.076	0.095	0.092
Triangular	Long 2	0.044	0.092	0.092	0.097	0.102	0.114	0.114	0.119	0.122
Triangular	Ponytail	0.044	0.080	0.080	0.077	0.078	0.107	0.105	0.116	0.152
Triangular	Updo 1	0.026	0.064	0.064	0.067	0.075	0.089	0.087	0.104	0.130
Triangular	Updo 2	0.043	0.093	0.093	0.099	0.111	0.132	0.131	0.152	0.181
Triangular	Med-Len	0.062	0.114	0.114	0.120	0.127	0.145	0.145	0.147	0.150
Widow's Peak	Short	0.047	0.089	0.089	0.092	0.084	0.099	0.098	0.106	0.106
Widow's Peak	Dreadlocks	0.028	0.047	0.047	0.047	0.043	0.051	0.051	0.048	0.049
Widow's Peak	Spiky	0.043	0.107	0.107	0.120	0.129	0.126	0.128	0.129	0.132
Widow's Peak	Side fringe	0.052	0.125	0.125	0.146	0.156	0.121	0.118	0.137	0.129
Widow's Peak	Long 1	0.032	0.066	0.066	0.077	0.092	0.092	0.090	0.103	0.104
Widow's Peak	Long 2	0.019	0.034	0.034	0.034	0.032	0.047	0.047	0.050	0.049
Widow's Peak	Ponytail	0.032	0.069	0.069	0.072	0.068	0.075	0.074	0.072	0.089
Widow's Peak	Updo 1	0.029	0.059	0.059	0.066	0.090	0.076	0.075	0.073	0.082
Widow's Peak	Updo 2	0.039	0.057	0.057	0.065	0.116	0.058	0.058	0.061	0.092
Widow's Peak	Med-Len	0.033	0.052	0.052	0.055	0.051	0.059	0.059	0.065	0.063

Table 2: Quantitative errors of the hair-root density changes. For 10 hairstyles with 6 hairline edits, our method produces *consistent* results under four different parameterization algorithms, i.e., LSCM [4], Harmonic map [2], ARAP [6], and the one introduced in [3].

Hairline	Hairstyle	$\ \cdot\ _1$ of density change				$\ \cdot\ _\infty$ of density change			
		LSCM	Harmonic	ARAP	Scalp	LSCM	Harmonic	ARAP	Scalp
Straight	Short	0.041	0.041	0.041	0.042	0.344	0.344	0.346	0.338
Straight	Dreadlocks	0.024	0.024	0.024	0.024	0.493	0.493	0.494	0.473
Straight	Spiky	0.040	0.040	0.041	0.041	0.439	0.438	0.504	0.703
Straight	Side fringe	0.046	0.046	0.046	0.046	0.438	0.439	0.485	0.498
Straight	Long 1	0.040	0.040	0.040	0.039	0.363	0.363	0.366	0.348
Straight	Long 2	0.015	0.015	0.015	0.015	0.279	0.279	0.276	0.258
Straight	Ponytail	0.033	0.033	0.033	0.033	0.405	0.405	0.419	0.783
Straight	Updo 1	0.036	0.036	0.036	0.039	1.023	1.023	1.018	2.084
Straight	Updo 2	0.048	0.048	0.048	0.048	0.460	0.459	0.422	0.595
Straight	Med-Len	0.028	0.028	0.028	0.028	0.323	0.323	0.324	0.318
Bell-shaped	Short	0.034	0.034	0.034	0.034	0.404	0.404	0.406	0.401
Bell-shaped	Dreadlocks	0.038	0.038	0.038	0.038	0.377	0.377	0.359	0.406
Bell-shaped	Spiky	0.046	0.046	0.046	0.046	0.460	0.460	0.452	0.452
Bell-shaped	Side fringe	0.058	0.058	0.059	0.059	0.797	0.798	0.755	1.103
Bell-shaped	Long 1	0.078	0.078	0.078	0.078	0.532	0.565	0.515	0.732
Bell-shaped	Long 2	0.045	0.045	0.045	0.045	0.457	0.458	0.515	0.891
Bell-shaped	Ponytail	0.062	0.062	0.062	0.063	0.450	0.450	0.450	2.443
Bell-shaped	Updo 1	0.075	0.075	0.075	0.075	0.744	0.743	0.721	0.860
Bell-shaped	Updo 2	0.091	0.091	0.091	0.091	0.587	0.586	0.537	0.821
Bell-shaped	Med-Len	0.049	0.049	0.049	0.049	0.397	0.397	0.394	0.401
Uneven	Short	0.050	0.050	0.050	0.050	0.349	0.349	0.342	0.342
Uneven	Dreadlocks	0.041	0.041	0.041	0.040	0.855	0.854	0.815	0.468
Uneven	Spiky	0.045	0.045	0.045	0.044	1.566	1.558	1.784	0.800
Uneven	Side fringe	0.043	0.043	0.043	0.043	0.447	0.447	0.466	0.391
Uneven	Long 1	0.021	0.021	0.021	0.021	0.374	0.374	0.379	0.357
Uneven	Long 2	0.034	0.034	0.034	0.034	0.835	0.834	0.690	0.356
Uneven	Ponytail	0.040	0.040	0.040	0.041	0.408	0.408	0.421	0.781
Uneven	Updo 1	0.017	0.017	0.017	0.019	0.985	0.985	0.973	1.728
Uneven	Updo 2	0.029	0.029	0.029	0.028	0.461	0.460	0.424	0.465
Uneven	Med-Len	0.050	0.050	0.050	0.050	0.640	0.639	0.656	0.418
M-shape	Short	0.046	0.046	0.046	0.046	0.584	0.583	0.592	0.617
M-shape	Dreadlocks	0.032	0.032	0.032	0.032	0.472	0.472	0.473	0.452
M-shape	Spiky	0.037	0.037	0.037	0.037	0.418	0.416	0.432	0.434
M-shape	Side fringe	0.048	0.048	0.048	0.047	1.057	1.056	1.052	0.964
M-shape	Long 1	0.025	0.025	0.025	0.025	0.592	0.592	0.584	0.588
M-shape	Long 2	0.027	0.027	0.027	0.027	0.280	0.280	0.277	0.259
M-shape	Ponytail	0.037	0.037	0.037	0.038	0.413	0.413	0.422	0.795
M-shape	Updo 1	0.026	0.026	0.026	0.026	0.979	0.979	0.961	1.785
M-shape	Updo 2	0.032	0.032	0.032	0.031	0.460	0.460	0.421	0.465
M-shape	Med-Len	0.041	0.041	0.041	0.041	0.324	0.324	0.326	0.319
Triangular	Short	0.053	0.053	0.053	0.053	1.150	1.148	1.243	0.988
Triangular	Dreadlocks	0.051	0.051	0.051	0.050	2.641	2.637	2.608	2.170
Triangular	Spiky	0.046	0.046	0.046	0.046	1.919	1.915	1.956	2.011
Triangular	Side fringe	0.034	0.034	0.034	0.034	0.516	0.514	0.483	0.591
Triangular	Long 1	0.024	0.024	0.024	0.024	0.516	0.516	0.495	0.525
Triangular	Long 2	0.044	0.044	0.045	0.044	2.220	2.218	2.057	1.790
Triangular	Ponytail	0.044	0.044	0.044	0.045	1.082	1.082	0.985	1.360
Triangular	Updo 1	0.026	0.026	0.026	0.026	1.417	1.416	1.556	2.488
Triangular	Updo 2	0.043	0.043	0.043	0.044	1.556	1.555	1.598	1.746
Triangular	Med-Len	0.062	0.062	0.062	0.062	1.767	1.766	1.955	1.583
Widow's Peak	Short	0.047	0.047	0.047	0.047	0.366	0.366	0.352	0.363
Widow's Peak	Dreadlocks	0.028	0.028	0.028	0.028	0.481	0.481	0.482	0.462
Widow's Peak	Spiky	0.043	0.043	0.043	0.043	0.359	0.359	0.374	0.391
Widow's Peak	Side fringe	0.052	0.052	0.052	0.052	0.438	0.439	0.456	0.399
Widow's Peak	Long 1	0.032	0.032	0.032	0.032	0.365	0.365	0.369	0.347
Widow's Peak	Long 2	0.019	0.019	0.019	0.018	0.280	0.280	0.277	0.259
Widow's Peak	Ponytail	0.032	0.032	0.032	0.033	0.409	0.409	0.421	0.795
Widow's Peak	Updo 1	0.029	0.029	0.029	0.030	0.991	0.991	0.973	1.990
Widow's Peak	Updo 2	0.039	0.039	0.039	0.039	0.460	0.459	0.421	0.466
Widow's Peak	Med-Len	0.033	0.033	0.033	0.033	0.324	0.324	0.326	0.319

Table 3: Quantitative comparisons of the multi-scale and global solving strategies. We list the $E_{\text{inter-strand}}$ values. This energy reaches a large value when ISR preservation is not incorporated. Our multi-scale solving produces much lower values, which are close to the global solving.

Hairstyle	w/o ISR preservation	Multi-scale solving	Global solving
Short	9.20×10^{-3}	3.34×10^{-3}	1.65×10^{-3}
Dreadlocks	2.55×10^{-1}	7.03×10^{-2}	2.56×10^{-2}
Spiky	2.58×10^{-2}	1.26×10^{-2}	5.61×10^{-3}
Side fringe	1.14×10^{-1}	3.96×10^{-2}	1.39×10^{-2}
Long 1	$1.93 \times 10^{+1}$	8.68×10^{-1}	1.29×10^{-1}
Long 2	$3.41 \times 10^{+1}$	5.78×10^{-1}	1.98×10^{-1}
Ponytail	4.93×10^{-1}	9.11×10^{-2}	1.54×10^{-2}
Updo 1	5.67×10^{-1}	1.27×10^{-1}	3.54×10^{-2}
Updo 2	5.16×10^{-1}	7.59×10^{-2}	2.30×10^{-2}
Med-Len	$3.26 \times 10^{+0}$	2.36×10^{-1}	5.56×10^{-2}

Table 4: Quantitative energy values of the ablation study. We compute each energy term on the transfer results with/without incorporating this term into the optimization. We report the values for all the hairstyles we used.

Hairstyle	$E_{\text{strand-shape}}$ (SS)		$E_{\text{hair-body}}$ (HBR)		$E_{\text{inter-strand}}$ (ISR)	
	opt with SS	opt w/o SS	opt with HBR	opt w/o HBR	opt with ISR	opt w/o ISR
Short	20.035	88.870	0.3942	0.5033	0.1093	0.1333
Dreadlocks	75.991	344.07	0.8612	9.5976	0.3131	0.5682
Spiky	52.450	252.04	0.9843	1.4441	0.1898	0.2243
Side fringe	65.133	214.68	1.3219	2.2503	0.2549	0.4103
Long 1	430.49	859.24	15.757	47.093	1.7761	9.0266
Long 2	246.62	402.95	4.5798	18.808	0.7965	1.6422
Ponytail	178.22	297.17	3.6629	18.583	0.6319	2.4922
Updo 1	189.12	334.77	3.7159	19.803	0.5800	1.0801
Updo 2	446.76	876.16	20.707	75.386	1.6359	14.390
Med-Len	382.76	853.88	11.652	34.215	1.1548	4.8966



Figure 6: Comparison of our retargeting method with the 3D RBF transfer method. The transfer results with 3D RBF method exhibit incorrect inter-strand and hair-body relationships, especially for the hair particles far away from the scalp. We fit the 3D RBF model based on the hair-root positions and apply it to the whole hairstyle.



Figure 7: Comparison of our retargeting method with the rigid transfer method. For rigid transfer, we compute a global rotation between the source and target head, as well as local translations for each strand based on their root positions on the scalp, which are determined by the barycentric coordinates. The transfer results with rigid transfer exhibit incorrect shapes and artifacts in many places.

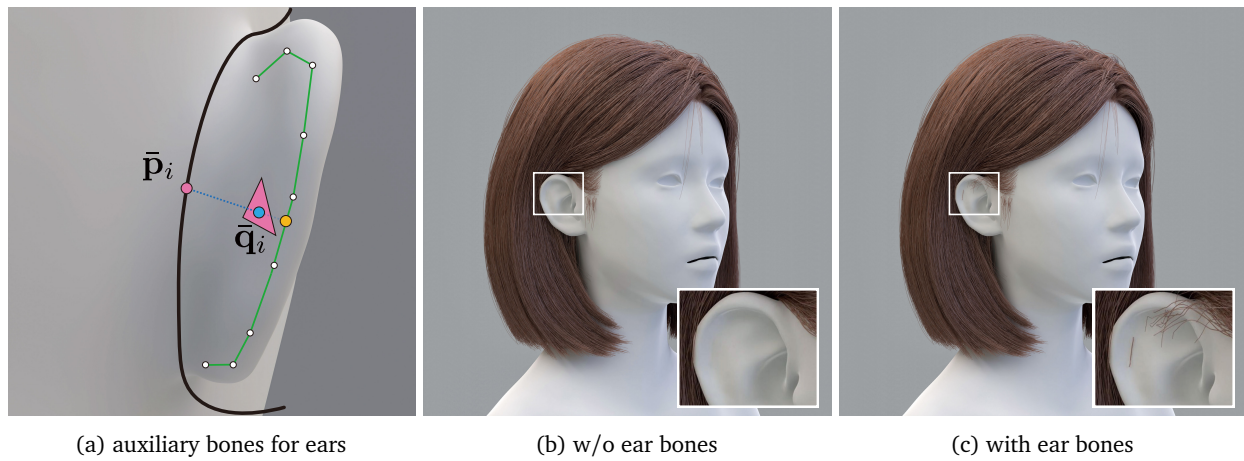


Figure 8: (a) Auxiliary bones for ears. (b) Transfer result without auxiliary bones for ears. (c) Transfer result with auxiliary bones for ears.

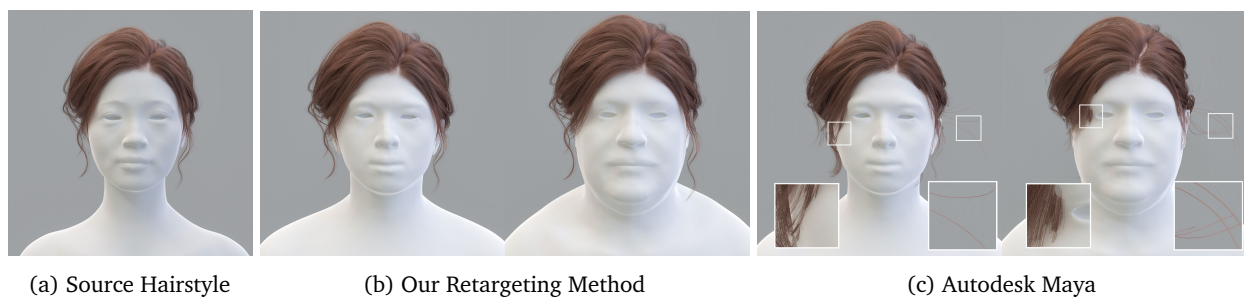


Figure 9: Comparison of our retargeting method with the *Transfer* command of Maya [5].